Nonlinear electrokinetic phenomena

Synonyms

Induced-charge electro-osmosis (ICEO), induced-charge electrophoresis (ICEP), AC electro-osmosis (ACEO), electro-osmosis of the second kind, electrophoresis of the second kind, Stotz-Wien effect, nonlinear electrophoretic mobility.

Definition

Nonlinear electrokinetic phenomena are electrically driven fluid flows or particle motions, which depend nonlinearly on the applied voltage. The term is also used more specifically to refer to induced-charge electro-osmotic flow, driven by an electric field acting on diffuse charge induced near a polarizable surface.

Chemical and Physical Principles

Linear electrokinetic phenomena

A fundamental electrokinetic phenomenon is the electro-osmotic flow of a liquid electrolyte (solution of positive and negative ions) past a charged surface in response to a tangential electric field. Electrophoresis is the related phenomenon of motion of a colloidal particle or molecule in a background electric field, propelled by electro-osmotic flow in the opposite direction. The basic physics is as follows:

Electric fields cause positive and negative ions to migrate in opposite directions. Since each ion drags some of the surrounding fluid with it, any significant local charge imbalance yields an electrostatic stress on the fluid. Ions also exert forces on each other, which tend to neutralize the bulk solution, so electrostatic stresses are greatest in the electrical double layers, where diffuse charge exists to screens surface charge. The width of the diffuse part of the double layer (or "diffuse layer") is the Debye screening length ($\lambda \sim$ 1-100 nm in water), which is much smaller than typical length scales in microfluidics and colloids. Such a "thin double layer" resembles a capacitor skin on the surface.

Electro-osmosis produces an effective slip of the liquid outside the double layer past to the solid surface. In the classical continuum model of the diffuse layer, the slip velocity is given by the Helmholtz-Smoluchowski formula,

$$u_s = -\frac{\varepsilon \zeta}{\eta} E_t \qquad [1]$$

where E_t is the tangential electric field just outside the double layer, ε and η are the permittivity and viscosity of the liquid (both assumed constant), and ζ is the zeta potential, a measure the electro-osmotic mobility with units of voltage. In Smoluchowski's theory, the zeta potential corresponds to the potential difference ψ between the slip plane and the neutral bulk solution, just outside the double layer, but this need not be the case (see below).

Classical electrokinetic phenomena are *linear* ($u \propto E$) since the zeta potential is assumed to be a material constant, reflecting chemical equilibrium at the liquid-solid interface:

$$u = -\frac{\varepsilon\zeta}{\eta} E = -bE \qquad \text{(non-polarizable surface)} \qquad [2]$$

The electro-osmotic mobility b is the coefficient of linear response. This ubiquitous approximation, which can be justified in the limits of thin double layers and/or weak fields, greatly limits possible flows and particle motions. With constant zeta and thin double layers, for example, electro-osmosis in a capillary is irrotational (free of vortices), and particles of different shapes and sizes have the same electrophoretic mobility $b = U/E$ and thus cannot be separated.

Induced-charge electrokinetic phenomena

The possibility of *nonlinear* electro-osmotic flow, varying as $u \propto E^2$, seems to have been first described by Murtsovkin (1,16), who showed that an alternating electric field can drive steady quadrupolar flow around a polarizable particle (Figure 1a). This effect has recently been unified with other nonlinear electrokinetic phenomena in microfluidics (2), such as AC electro-osmotic flow (ACEO) at microelectrodes (11,12,4) (Figure 1b), DC electrokinetic jets at dielectric corners (5) (Figure 1c), and nonlinear flows around metal posts (3) (Figure 1d-e). These are all cases of induced-charge electro-osmosis (ICEO) – the nonlinear electro-osmotic flow resulting from the action of an electric field on its own induced diffuse charge near a polarizable surface.

The simplest example of ICEO involves a metal sphere (1) or cylinder (2) in a suddenly applied field, sketched in Figure 2. Conceptually, there two steps: electrochemical relaxation in response to the field, and electro-osmotic flow driven the induced charge.

1. *Charge relaxation*. When the field is turned on, electrons on the metal surface immediately drift toward one pole to induce a dipole moment making the surface equipotential (Figure 2a). This is an unsteady configuration in an electrolyte, however, since the field drives ionic current, any normal component transports charge in or out of the diffuse layer. Ignoring surface conduction through the double layer (for thin double layers) and Faradaic reactions passing current through the particle (at low voltage), the normal current locally charges double layer, like a capacitor, until all the field lines are expelled in steady state (Figure 2b). The time scale for this process is the "RC time" for the equivalent circuit of the bulk resistance coupled to the double layer capacitance (12,2-4)

$$\tau = \frac{L}{\sigma} \frac{C_D}{(1+\delta)} = \frac{\lambda L}{D(1+\delta)} \qquad [3]$$

where $\delta = C_D/C_S$ is the ratio of the diffuse-layer capacitance to that of the compact layer (e.g. a Stern monolayer or dielectric coating), σ and D are the bulk conductivity and diffusivity, and L is the length (radius) of the object. In microfluidic devices, the double layer charging time [3] (ms) is much larger than the Debye relaxation time $\varepsilon/\sigma = \lambda^2/D$ for bulk ionic screening (μs) and much smaller than the diffusion time L^2/D for the relaxation of bulk concentration gradients (s). In nano-channels, however, all of these time scales can be comparable (μs).

2. *Fluid flow*. The tangential field acts on the non-uniform induced-charge (or ζ) distribution to produce quadrupolar ICEO flow, sucking fluid at the poles and ejecting it at the equator (Figure 2c). The scaling of the flow can be easily understood as

follows. Capacitive charging transmits a non-uniform voltage to the double layer of order *EL,* a fraction $(1+\delta)^{-1}$ of which is dropped across the diffuse part and contributes to the induced zeta potential. If [2] holds, then ICEO flow scales as

$$u \propto \frac{\varepsilon L E^2}{\eta(1+\delta)} \qquad \text{(ideally polarizable surface)} \qquad [4]$$

The flow builds up over the time scale τ in [3]; if an AC field of frequency ω is aplied, then the flow decays above the RC frequency as $[1+(\omega\tau)^2]^{-1}$, assuming constant double-layer capacitance (3).

In this canonical example, broken symmetries generally lead to fluid flow past the object, if it is held fixed, or motion by induced-charge electrophoresis (ICEP), if it is freely suspended (2,17). For example, if the object has a nonzero total charge, then the ICEO flow is superimposed on the familiar streaming flow of linear electrophoresis (Figure 2d). Whenever [2] holds, the two effects are additive, since the total charge corresponds to a constant ζ offset, relative to the background potential. In fixed-potential ICEO (Figure 3b), the potential of a conductor controlled so as to induce total charge in phase with a (steady or oscillating) background field (3). The effective *L* in [4] is then set by the distances between the object and the electrodes supplying the background field, so fixed-potential ICEO flow can be much faster than the quadrupolar ICEO flow and has a different frequency response.

Other broken symmetries include irregular shapes (e.g. rods, polyhedra, etc.), non-uniform surface properties (e.g. partial dielectric or metallic coatings), and non-uniform background electric fields (17). In each case, net pumping of the fluid by ICEO results if the object is held fixed, which requires a certain force and torque. Conversely, if the object is a colloidal particle, then broken symmetries cause it to translate and rotate ICEP, as described in companion articles on the electrokinetic motion of polarizable particles and heterogeneous particles.

Nonlinear electrokinetic phenomena involving dielectrics

The example above assumes an "ideally polarizable" metal surface, where the double layer charges capacitively to sustain the entire voltage applied to the object, but the phenomenon of ICEO is much more general and occurs at any polarizable surface, to varying degrees (1-3). For example, if the metal object described above has a thin dielectric coating of width *h* and permittivity ε_d, then the quadrupolar ICEO flow scales as [3-4] with $\delta = (\varepsilon/\varepsilon_d)(h/\lambda)$. This shows that dielectric coatings, which are thicker than the Debye length, can substantially reduce ICEO flows at metal surfaces. In the opposite limit of a purely dielectric object of length $L >> \lambda$, the flow scales as

$$u \propto \frac{\varepsilon_d \lambda E^2}{\eta} \qquad \text{(dielectric surface)} \qquad [5]$$

which is smaller than for an ideally polarizable object [4] by a factor $(\varepsilon_d/\varepsilon)(\lambda/L)$.

Although often small, ICEO flows at dielectric surfaces need not be negligible in microfluidic devices, due to large local fields. For example, an electric field passing around a sharp corner in a dielectric microchannel can drive a strong "nonlinear electrokinetic jet" of ICEO flow due

to the corner field singularity (5), as shown in Figure 1b. In very simple terms, this phenomenon can be understood as half of the quadrupolar flow around a polarizable particle, where the jet corresponds to the outward flow at the equator in Figure 2c.

Dielectric objects can also experience electrostatic forces. The uniform component of a background electric field induces a dipole on the object, which then feels a torque to align it with the field. A field gradient can also apply a force to the induced dipole. Higher-order multipoles in the background field can likewise cause forces and torques by acting on higher-order induced multipole moments on the object. In the case of colloidal dielectric particles, these forces and torques (balanced by hydrodynamic drag) produce translation $u \propto \varepsilon L^2 \nabla E^2/\eta$ and rotation $\Omega \propto \varepsilon E^2/\eta$, respectively. This general effect, known as *dielectrophoresis* (DEP), is perhaps the best-known nonlinear electrokinetic phenomenon. The theory of DEP has mostly been developed for dielectric liquids, but in electrolytes, however, ICEO flows also occur, with the same scalings. The net electrokinetic motion of polarizable particles results from a competition between DEP and ICEP.

Nonlinear electrophoretic mobility

Prior to the discovery of ICEO flow in the 1980s, the possibility of field-dependent electrophoretic mobility for charged, polarizable particles was demonstrated by several groups in the 1970s (14,15). A theory predicting an E^2 correction to the mobility of a highly charged particle was first proposed by Simonova and Dukhin in 1976:

$$b(E) = \frac{U(E)}{E} \sim \frac{\varepsilon}{\eta}\left(\zeta + \alpha(Ea)^2 + ...\right) \qquad [6]$$

It has recently been proposed to refer to this nonlinear correction as the Stotz-Wien effect (14). As shown by AS Dukhin, it can be understood as a phenomenon of induced-charge electrophoresis due to the nonlinear differential capacitance $C(\psi)$ of the diffuse layer, as a function of its voltage drop ψ, given by $\psi = (\phi - \phi_{surface})/(1+\delta)$. The basic idea is that the redistribution of diffuse charge around a polarizable particle, which is induced in response to an applied field, leads to a shift of its potential $\phi_{surface} \propto E^2$, and thus of its electrophoretic mobility, in order to maintain the same total charge with a non-constant $C(\psi)$.

In principle, the Stotz-Wien effect can be used to separate colloidal particles using an unbalanced AC field, which has zero time average $\langle E \rangle = 0$, but nonzero time-averaged higher moments, such as $\langle E^3 \rangle \neq 0$. An unbalanced AC field leads to a size-dependent nonlinear electrophoretic velocity for a highly charged polarizable particle

$$\langle U \rangle = \alpha \frac{\varepsilon a^2}{\eta} \langle E^3 \rangle \qquad \text{(highly charged, polarizable particle)} \qquad [7]$$

This method of particle separation was first proposed by Chimenti in a U.S. patent (5,106,648, filed in 1985) and independently in Ukraine by Dukhin's group, who called the technique "aperiodic electrophoresis," around the same time (14).

Electrokinetic phenomena of the second kind

All of the examples above involve "blocking" surfaces, which do not pass any electrical current. If current can enter the surface, e.g. due to Faradaic reactions at a metal electrode or ionic conduction through a perm-selective porous material, then ICEO flows can be substantially modified. Electrical conduction through the surface tends to "short-circuit" the capacitive charging mechanism, so time-dependent ACEO flows tend to be reduced by Faradaic reactions. If a steady DC voltage is applied, then current into a surface can deplete the bulk salt concentration, leading to concentration polarization (breakdown of Ohm's law) and diffusio-osmosis (slip driven by bulk concentration gradients). If the current is large enough to nearly deplete the bulk concentration, at the diffusion-limited current, then the diffuse-charge in the electrical double layer loses thermal equilibrium and expands into the bulk. A super-limiting current causes the formation of extended space charge, which can alter the nature of ICEO flow.

The possibility of nonlinear electro-osmotic flow driven by non-equilibrium space charge at large currents was predicted by S.S. Dukhin in the 1980s (13,6). He coined the term electro-osmosis of the second kind, to distinguish it from electrokinetic phenomena of the first kind (whether linear or nonlinear), which involve quasi-equilibrium double layers and non-zero bulk concentrations. In spite of appealing to very different physical mechanisms, the maximum velocity of second-kind electro-osmosis is argued to be the same as that described above for ICEO flow [4]:

$$u \propto \frac{\varepsilon L E^2}{\eta} \qquad \text{(surface at limiting current)} \qquad [8]$$

The reason is that in both cases the applied voltage is transferred to a charged layer near the surface as an induced zeta potential, $\zeta_{induced} \approx EL$, either by space charge formation at large currents or by capacitive charging of the diffuse layer, respectively.

In spite of similar scaling, electro-osmosis of the second kind is fundamentally different from ICEO flow below a limiting current. Second-kind electro-osmosis requires near-total depletion of the bulk salt concentration by a large current, so it arises at the slow time scale of bulk diffusion, L^2/D, which is much greater than the capacitive double-layer charging time [3]. It is essentially a DC effect. The passage of current through the surface also breaks symmetry in a different way in the electrokinetic motion of polarizable particles by electrophoresis of the second kind. For example, if the particle in Figure 2c could pass a large current of counterions, then only its lower portion (facing the field) would form space charge and drive second-kind flow propelling the particle toward the field (roughly half of the quadrupolar flow field of ICEO). This picture is oversimplified, however, since experimentally observed second-kind flows can be more complicated, as sketched in Figure 3 (6).

Space charge formation and second-kind electro-osmosis can also be observed in microfluidic devices and porous materials at interfaces between nanochannels and microchannels, as sketched in Figure 4 (7). Nano-scale pores with overlapping double layers act as filters, allowing the passage of only counterions. The applied electric field drives a current, which can be strong enough to deplete the nearby bulk salt concentration, resulting in a nonequilibrium space-charge layer of counterions. Tangential electric fields near the nanopore opening can then drive (often chaotic) second-kind flows in the surrounding micro-pore.

Other nonlinear electrokinetic phenomena

Induced-charge and second-kind electrokinetic phenomena arise due to electrohydrodynamic effects in the electric double layer, but the term "nonlinear electrokinetic phenomena" is also sometimes used more broadly to include any fluid or particle motion, which depends nonlinearly on an applied electric field. In the classical effect of dielectrophoresis mentioned above, electrostatic stresses on a polarized dielectric particle in a dielectric liquid cause dielectrophoretic motion of particles and cells along the gradient of the field intensity ($\propto \nabla E^2$). In electrothermal effects, an electric field induces bulk temperature gradients by Joule heating, which in turn cause gradients in the permittivity and conductivity that couple to the field to drive nonlinear flows, e.g. via Maxwell stresses $\propto E^2 \nabla \varepsilon$. In cases of flexible solids and emulsions, there can also be nonlinear electro-mechanical effects coupling the motions of different fluid and/or solid phases, driven by electric fields. Electric fields applied to diffuse interfaces between liquid phases, e.g. at different salt concentrations, can also produce electrokinetic flow instability, which depends nonlinearly on the field amplitude through the electric Rayleigh number ($\propto E^2 \nabla \sigma$). All of these nonlinear electrokinetic phenomena can further be modified by the simultaneous application of a magnetic field, which drives fluid flow and particle motion due to the Lorentz force ($J \times B$) acting on ionic currents in solution.

Key Research Findings

Induced-charge electrokinetic phenomena

The first experiments demonstrating field-dependent electrophoretic mobility of colloids (Stotz-Wien effect) were reported by several groups in the 1970s (14), and the possibility of using this effect for particle separation using unbalanced AC fields has begun to be explored (14). This work focused on nonlinear corrections to the classical phenomenon of electrophoresis, where a particle moves in the direction of the applied electric field, $U = b(E)E$, rather than on the associated ICEO flows and more complicated ICEP motion.

In a series of pioneering experiments on polarizable colloids, Murtsovkin and collaborators studied ICEO flows around tin, quartz, and ionite particles and liquid mercury drops in alternating electric fields and compared with the theory (1). The scalings of the fundamental quadrupolar flow with the electric field squared and the particle size [4] were roughly verified (e.g. Figure 5a), although in some cases the flow was observed in the opposite direction from the theory, at large induced voltages. The electrokinetic motion of polarizable particles and heterogeneous particles by ICEP has also begun to be observed and analyzed in experiments, including unusual motion perpendicular to a uniform AC field, but much remains to be done.

Detailed three-dimensional measurements of ICEO flows are now possible in microfluidic devices. Using particle-image velocimetry applied to thin optical slices, the ICEO flow field around a platinum cylinder has recently been reconstructed experimentally (Figure 5b) and found to agree well with the theory, up to a scaling factor which could perhaps be attributable to compact-layer effects (8). There has also been extensive experimental work on AC electro-osmotic flows in microfluidic devices, discussed in a separate article.

Experiments lend some support to the simplest theory of ICEO, used in nearly all calculations, which describes the bulk as an Ohmic resistor coupled to thin double layer capacitors. The mathematical model consists of Laplace's equation for the bulk

electrostatic potential, $\nabla^2\phi = 0$, with an "RC" boundary condition equating the change in diffuse-layer charge density with the current entering from the bulk solution,

$$C(\psi)\frac{d\psi}{dt} = n\cdot(\sigma\nabla\phi) \qquad [9]$$

Once the electrochemical problem is solved, the ICEO flow is obtained by solving Stokes' equations, $\nabla p = \eta\nabla^2\vec{u}$ and $\nabla\cdot\vec{u} = 0$, with electro-osmotic slip given by [1] with the induced zeta potential, $\zeta = \psi$. Although this set of approximations can only be justified at low voltages in a dilute solution (3), it has had many successes in predicting induced-charge electrokinetic phenomena in experiments outside this regime.

There is, however, a need to extend the theory of ICEO to "large voltages", $\psi >> kT/e$, where the induced diffuse-layer potential greatly exceeds the thermal voltage (25 mV at room temperature). Experiments on AC electro-osmotic flows involve micro-elecrode arrays applying several volts ($\approx 100kT/e$), and indeed many features of the data cannot be explained by the low-voltage theory, such as flow reversal at high frequency and flow suppression with increasing salt concentration as $u \sim \log(c_{\max}/c)$ extrapolating to zero around 10 mM. Similarly, experiments on the electrokinetic motion of polarizable particles and heterogeneous particles at somewhat lower voltages also exhibit flow reversal and the same, seemingly universal concentration dependence.

The primary consequence of a large applied voltage is the crowding of counterions near a highly polarized surface, which violates the assumptions of the classical dilute solution theory. By considering steric constraints and increased viscosity due to counterion crowding, a modified electro-osmotic slip formula has recently been derived for large induced diffuse-layer voltages in a symmetric z:z electrolyte, where

$$\overline{\zeta} = \psi - \mathrm{sgn}(\psi)\frac{kT}{ze}\log\left[1 + 4\frac{c_{\max}}{c}\sinh^2\left(\frac{ze\psi}{2kT}\right)\right] \qquad [10]$$

is the apparent zeta potential in [1] and $c_{\max} = a^{-3}$ is a counterion concentration (charge density) where the viscosity is postulated to diverge (9). The critical separation a is at least the solvated ion radius, but could be effectively larger due to under-estimation of steric effects in this lattice-gas-based model and (poorly understood) correlation effects on the viscosity. This theory reduces to Smoluchowski's at low voltages ($\overline{\zeta} \sim \psi$ for $|\psi| << \psi_c$), but the electro-osmotic mobility saturates $\overline{\zeta} \sim \mathrm{sgn}(\psi)\psi_c$ at a concentration-dependent value,

$$\psi_c = \frac{kT}{ze}\log\left(\frac{c_{\max}}{c}\right) \qquad [11]$$

at large voltages $|\psi| >> \psi_c$. This model seems to qualitatively capture the basic features of ICEO flows in experiments, but a complete quantitative theory is still lacking. It may be necessary to go beyond the mean-field approximation (i.e. Poisson's equation for the electrostatic potential in the diffuse layer). Atomistic simulations and nano-scale

experiments should be crucial to guide the further development of a modified theory of ICEO at large applied voltages.

Electrokinetic phenomena of the second kind

There is growing body of experimental literature on nonlinear electro-osmotic flows around highly conductive, permselective ionite particles and porous structures in microfluidics (6-7). The basic velocity scaling [8] has been verified, and the time scale for the onset of the flow has been shown to be diffusive (L^2/D = minutes), not capacitive [3] (milliseconds). Imaging of second-kind flow around ionite particles with submicron tracers has shown that the largest electro-osmotic slip is near the surfaces sustaining the largest incoming current density, resulting in a flow profile around a spherical particle, which resembles a shifted dipole or the structure in Fig. 3. Space–charge formation and concentration gradients have also been directly imaged in porous structures using charged and neutral tracers.

The mathematical theory of electro-osmosis of the second kind is still in its infancy. Scaling arguments modifying [8] have been made to quantify various effects in second-kind electrophoresis, such as advection-diffusion (large Peclet number), but precise flow fields and particle motions have not yet been calculated (or even approximated) starting from the underlying nonlinear partial differential equations of electrochemical hydrodynamics. Mathematical modeling of space charge formation has also mostly been restricted to one-dimensional conduction (as in Figure 4).

An exception is the case of electrokinetic/hydrodynamic flow instability at electro-dialysis membranes, where mathematical modeling has recently implicated second-kind electro-osmosis as a likely mechanism for super-limiting current. Starting from the classical Poisson-Nernst-Planck and Navier-Stokes equations, Rubinstein and Zaltzman have shown that one-dimensional conduction is stable until the bulk concentration approaches zero at the classical Nernst limiting current, due to fast Faradaic reactions limited by bulk diffusion (10). In particular, hydrodynamic instability due to classical “first-kind” electro-osmotic and diffusio-osmotic flow does not occur. At the limiting current, the double layer expands, while remaining “thin” compared to the typical geometrical length scale, and assumes a non-equilibrium structure altered by the passage of normal current. In this thin space-charge layer, hydrodynamic instability occurs via second-kind electro-osmotic flows, and the resulting electro-convection brings concentrated fluid to the surface to enhance the reaction rate and exceed the diffusion-limited current.

A novel aspect of this theory is the derivation of a modified slip formula for second-kind electro-osmosis,

$$u_s = -\frac{\varepsilon V^2}{8\eta}\nabla_s \ln\left(\hat{n}\cdot\nabla c\right) \qquad \text{(surface at limiting current)} \qquad [12]$$

where V is the applied voltage on the surface (10). The slip is thus given by the surface gradient of the normal diffusive flux entering the space charge layer. A unified theory of electro-osmotic slip at all applied voltages has also been derived and applied to the problem of hydrodynamic instability at electro-dialysis membranes. However, it has not yet been applied to second-kind electro-osmotic flows in other experimental situations of electrophoresis and microfluidic devices.

In spite of the complications resulting from concentration gradients and normal current, the classical transport equations used in this analysis are likely to remain valid for second-kind electro-osmosis. The reason is that the normal current prevents the overcharging of the diffuse layer, and instead most of the voltage drop occurs in the extended space charge layer, where the counterion concentration is small (and the co-ion concentration is negligible). Complicated effects of ion crowding, which are crucial in induced-charge electrokinetics at large voltages (e.g. Eqs. [9-11]), are thus not important. This further underscores the difference between first-kind and second-kind induced-charge electrokinetic phemomena.

Examples of Applications

There are many applications of nonlinear electrokinetic phenomena in microfluidics. For example, the dielectrophoretic motion of particles and cells is used for separating and concentrating biological samples. Electrokinetic flow instability and electrothermal effects can be used for microfluidic mixing.

Induced-charge electrokinetic phenomena are finding many new applications as well. AC electro-osmotic flow is a promising means of microfluidic pumping and mixing in portable or implantable devices, since it requires low voltage and low power. ACEO has also been used in conjunction with DEP to trap, concentrate, and release particles and cells. Induced-charge electro-osmosis can also be used for mixing, due to easy electrical control of complex flow patterns in space and time. Induced-charge electrophoresis leads to complicated new behavior of polarizable colloids, e.g. perpendicular to an AC field, which can be exploited in new kinds of separations. In all of these cases, the use of relatively weak AC voltages, enabled by nonlinearity, is a major advantage over the large DC voltages required for linear electrokinetics, since it can greatly reduce unwanted Faradaic reactions, gas bubbles, electrode dissolution, and sample contamination.

Electrokinetic phenomena of the second kind have received mostly academic interest, but there may be important and unexpected applications. Already, second-kind electro-osmosis has been implicated as a mechanism for superlimiting current in electrodialysis. Space-charge formation at nanochannel/microchannel junctions has also been exploited to trap biomolecules, although in that case the flow is undesirable since it interferes with trapping. The speed of second-kind electrophoresis may be useful in separation or mixing, but the need to apply a large DC voltage may limit its applicability.

Cross-references

Aperiodic electrophoresis (def)
AC Electro-osmotic Flow
Dielectrophoresis
Dielectrophoretic Motion of Particles and Cells
Diffusiophoresis
Electrical Double Layers
Electrokinetic/Hydrodynamic Flow Instability
Electrokinetic Motion of Heterogeneous Particles
Electrokinetic Motion of Polarizable Particles
Electroosmotic Flow

Electro-osmosis of the second kind (def)
Electrophoresis of the second kind (def)
Electrophoresis
Electrothermal Effects
Induced-charge electro-osmosis (def)
Induced-charge electrophoresis (def)
Space charge (def)
Stotz-Wien effect (def)
Super-limiting current (def)
Unbalanced AC field (def)

Further Reading

1. Murtsovkin VA (1996) Nonlinear flows near polarized disperse particles. Colloid Journal 58: 341–349.
2. Bazant MZ & Squires TM (2004) Induced-charge electrokinetic phenomena: theory and microfluidic applications. Physical Review Letters 92: art. no. 066010.
3. Squires TM and Bazant MZ (2004) Induced-charge electro-osmosis. Journal of Fluid Mechanics 509: 217-252.
4. Green NG, Ramos A, Gonzalez A, Morgan H, and Castellanos A (2002) Fluid flow induced by nonuniform ac electric fields in electrolytes on microelectrodes. III. Observation of streamlines and numerical simulation. Physical Review E 66: art. no. 026305.
5. Thamida SK, Chang H-C (2002) Nonlinear electrokinetic ejection and entrainment due to polarization at nearly insulated wedges. Physics of Fluids 14: 4315-4328.
6. Rathore AS & Horvath C (1997) Capillary electrochromatography: theories on electroosmotic flow in porous media. Journal of Chromotagraphy A 781: 185-195.
7. Leinweber FC and Tallarek U (2004) Nonequilibrium electrokinetic effects in beds of ion-permselective particles. Langmuir 20: 11637-11648.
8. Levitan JA, Devasenathipathy S, Studer V, Ben Y, Thorsen T, Squires TM, and Bazant MZ (2005) Experimental observation of induced-charge electro-osmosis around a metal wire in a microchannel. Colloids and Surfaces A: Physicochemical and Engineering Aspects 267: 122-132.
9. Bazant MZ, Kilic MS, Storey B & Ajdari A (2007) Nonlinear electrokinetics at large applied voltages. Preprint. (http://www.arxiv.org/abs/cond-mat/0703035)
10. Zaltzman, B. & Rubinstein, I. (2007) Electro-osmotic slip and electroconvective instability. Journal of Fluid Mechanics 579: 173 – 226.
11. Ajdari, A (2000) Pumping liquids using asymmetric electrode arrays. Physical Review E 61: R45-R48.
12. Ramos, A., Morgan, H., Green, N. G., & Castellanos, A. (1999) AC electric-field-induced fluid flow in microelectrodes, Journal of Colloid and Interface Science 217: 420-422.
13. Dukhin SS (1991) Electrokinetic phenomena of the 2nd kind and their applications. Advances in Colloid and Interface Science 35: 173-196.
14. Dukhin AS & Dukhin SS (2005) Aperiodic capillary electrophoresis method using an alternating current electric field for separation of macromolecules. Electrophoresis 26: 2149-2153.
15. Dukhin AS (1993) Biospecific mechanism of double layer formation and peculiarities of cell electrophoresis. Colloids and Surfaces A: Physicochemical and Engineering Aspects 73: 29-48.

16. Gamayunov NL, Mursovkin VA & Dukhin AS (1986) Pair interactions of particles in electric field. 1. Features of hydrodynamic interaction of polarized particles. Colloid Journal of the USSR 48: 197-203.
17. Squires TM & Bazant MZ (2006) Breaking symmetries in induced-charge electro-osmosis. Journal of Fluid Mechanics 560: 65-101.

Figure Legends

Figure 1

Experimental photographs of induced-charge electro-osmosis, imaged by streaks of tracer particles. (a) Nonlinear flow around a 500 μm spherical ionite particle driven by a weak 10 V/cm 80 Hz background AC electric field. (by V. A. Murtsovkin, courtesy of A. S. Dukhin); (b) AC electro-osmosis at a pair of titanium electrodes applying a 2 V 100 Hz AC voltage (from (4)); (c) DC electrokinetic jet at a dielectric microchannel corner (from 5); (d) one roll of quadrupolar ICEO flow around a 100 μm cylindrical gold post in a 100 V/cm 300 Hz electric field and (e) fixed potential ICEO flow around a gold post connected to one electrode supplying the background AC field (by J. Levitan).

Figure 2

Physical mechanism for induced-charge electro-osmosis around an ideally polarizable metal cylinder in a suddenly applied electric field (from 2). (a) When the field is turned on, electronic charges relax to make the surface an equipotential, but the normal current drives double-layer charging. (b) After charging, the field lines are expelled by a nonuniform distribution of induced double-layer charge. (c) The tangential field acts on the induced charge to drive quadrupolar ICEO flow around a neutral cylinder. (d) If the cylinder has a nonzero total charge, then the dipolar flow of linear electrophoresis is superimposed on the quadrupole.

Figure 3

A sketch of electro-osmotic flow of the second kind around an ion-permselective particle from experiments (from 6).

Figure 4

Sketch of space charge formation and second-kind flow at the junction between a nanopore and a micropore in a microfluidic device or porous material (from 7). (a) In equilibrium, the micropore contains neutral electrolyte, while the nanopore has overlapping double layers containing mostly counterions. (b) When an electric field is applied, the nanopore conducts a current of counterions, which depletes the nearby salt concentration in the micropore, forming a bulk diffusion layer. (c) If the field is strong enough, the bulk concentration goes to zero, leading to space charge formation and second-kind electro-osmotic flow in the micropore.

Figure 5

Some experimental data on induced-charge electrokinetic phenomena. (a) The fluid velocity at different points around a tin particle in an AC field versus the applied electric field, demonstrating the quadratic scaling of [4] (from (1) and references therein). (b) The velocity profile at different voltages, measured by micro-particle-image velocimetry, in an optical slice above a platinum cylinder in a transverse AC field, plotted with the scaling [4] to demonstrate data collapse. The simulated streamlines are shown above. (from (8)).

AUTHOR

Title: Associate Professor of Applied Mathematics

Name: Martin Z. Bazant

Affiliation/Address:

Department of Mathematics and Institute for Soldier Nanotechnologies, Massachusetts Institute of Technology, Cambridge, MA 02139 USA

and

Ecole Superieure de Physique et Chimie Industrielles, 10 rue Vauquelin, 75231 Paris, France

Phone: (617) 253-1713

Fax: (617) 253-8911

E-mail: bazant@math.mit.edu

Figure 1

(a)

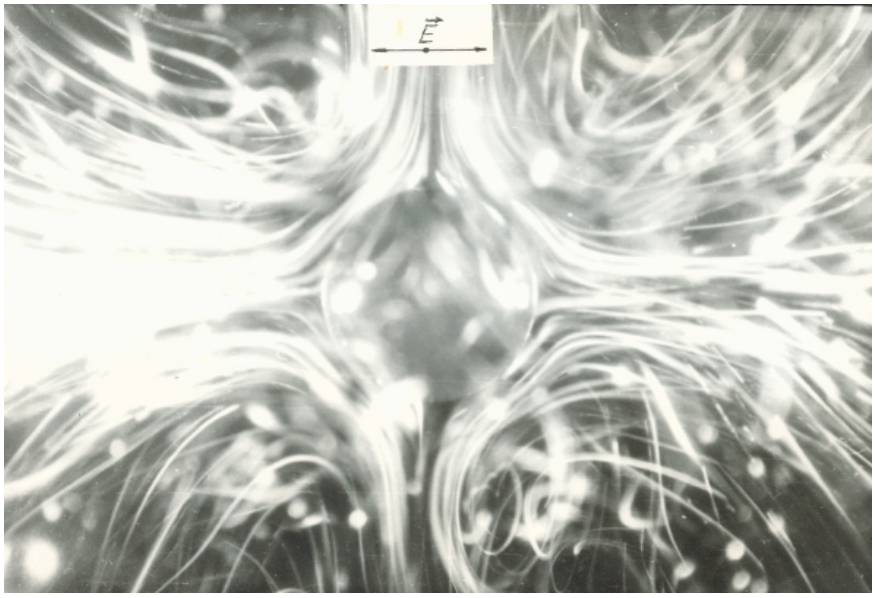

(b)

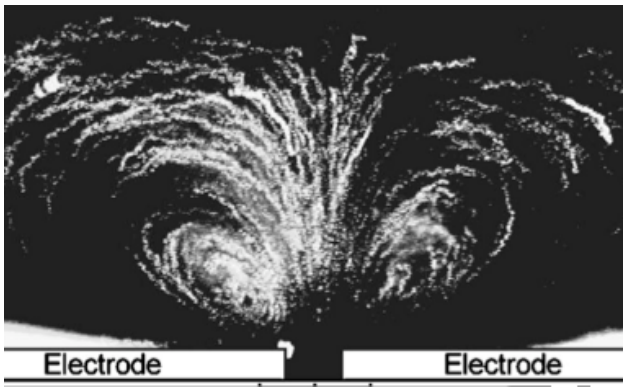

(c)

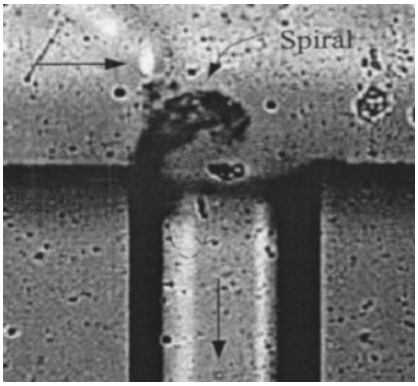

(d)

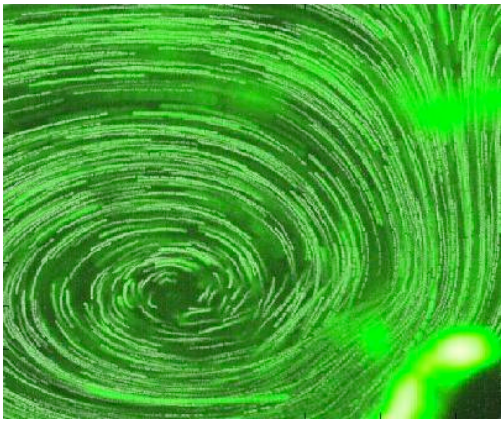

(e)

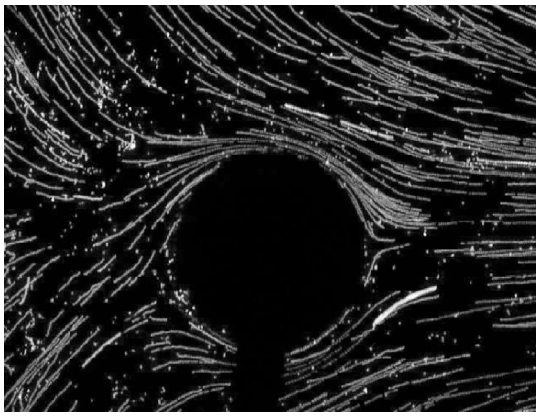

Figure 2

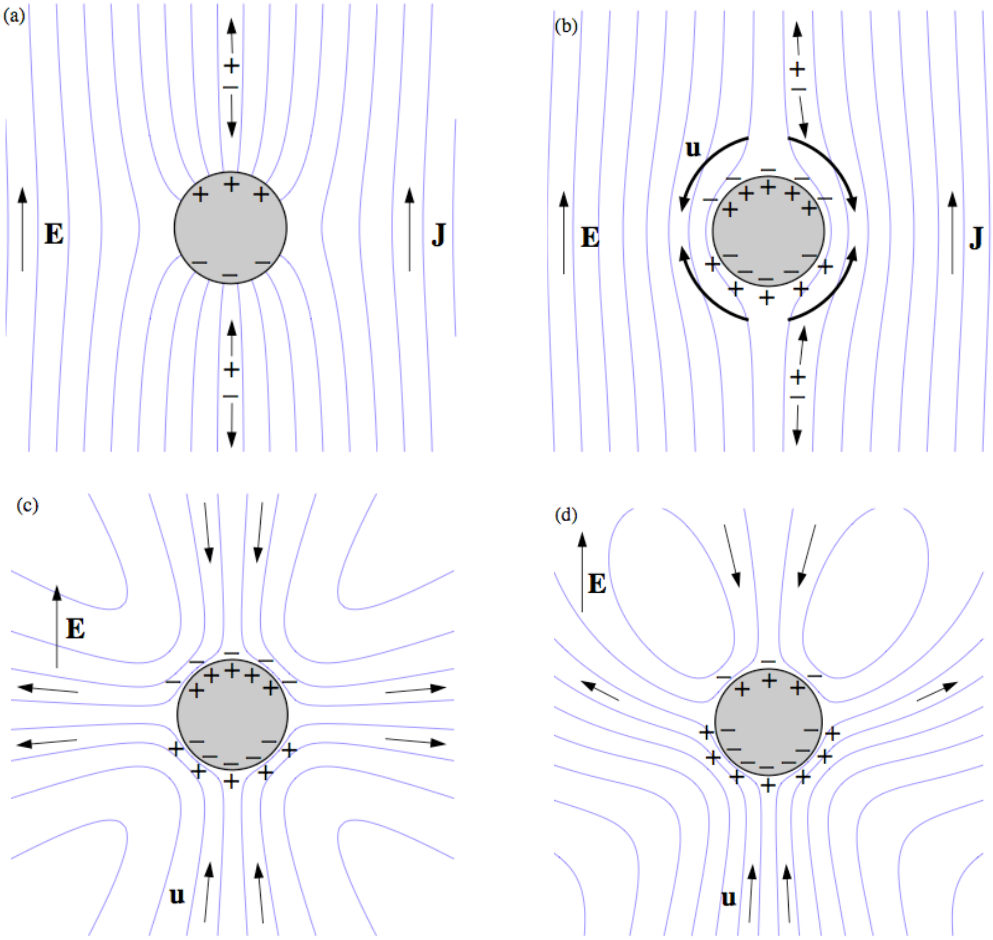

Figure 3

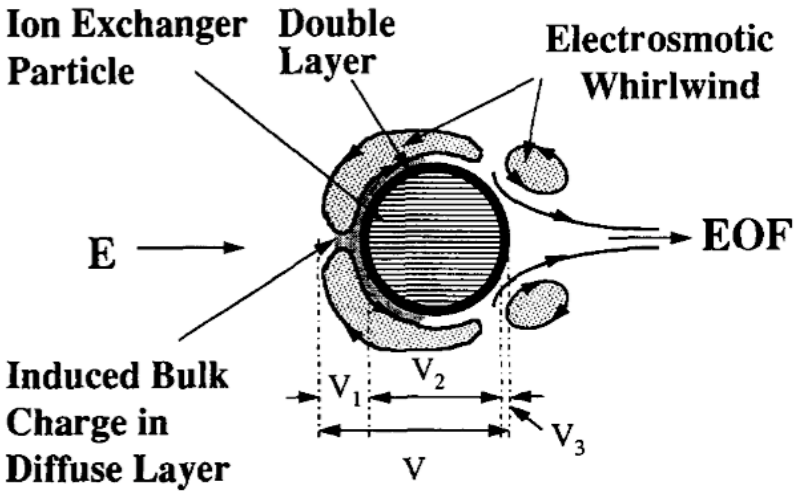

Figure 4

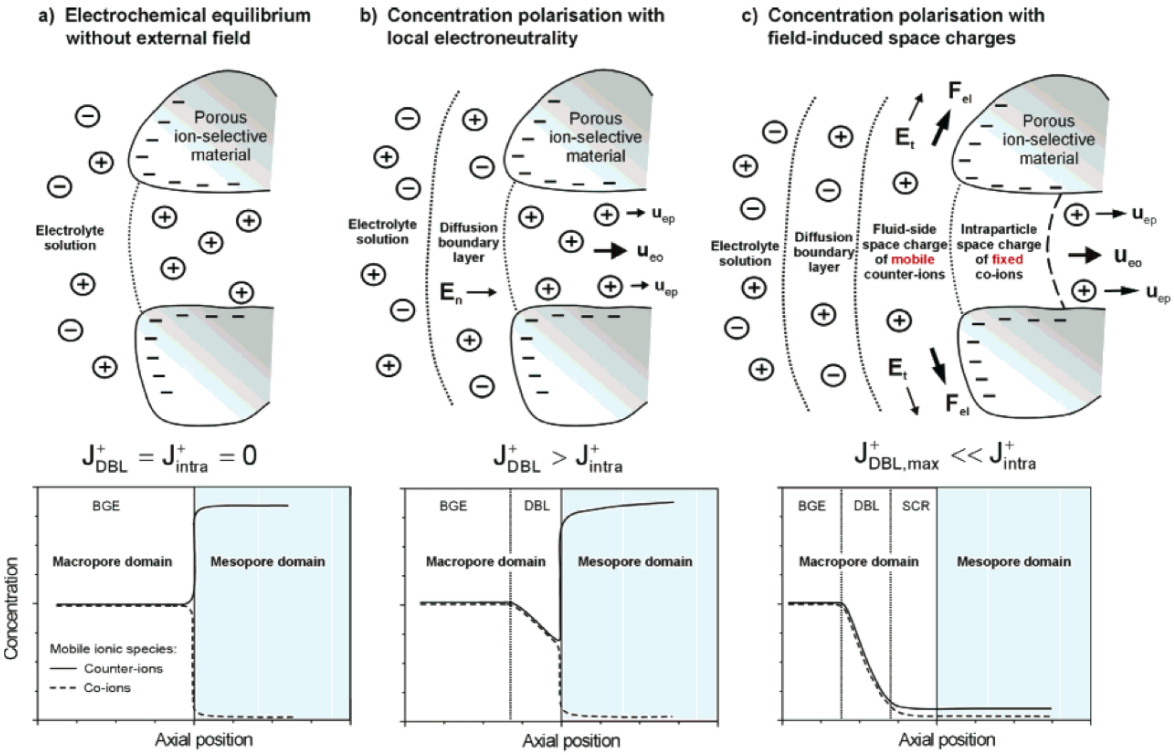

Figure 5